*Acta Cryst.* (1996). B52, 201–208

# Polymorphism of 7-Dimethylaminocyclopenta[*c*]coumarin: Packing Analysis and Generation of Trial Crystal Structures

A. GAVEZZOTTI

*Dipartimento di Chimica Strutturale e Stereochimica Inorganica, Università di Milano, via Venezian 21, 20133 Milano, Italy*

*(Received 15 May 1995; accepted 30 June 1995)*

## Abstract

The crystal structures of two polymorphs of the title compound [*Pbca* and $Pna2_1$; Jasinski & Woudenberg (1995). *Acta Cryst.* C51, 107–109] were analysed. Packing energies and indices were compared. Molecules in the two forms show a slight conformational difference; both conformers were packed in some of the most frequent space groups for organic molecules ($P2_1$, $P2_1/c$, $P2_12_12_1$ and $Pna2_1$) using a computer program for crystal structure generation and prediction (*PROMET*3). The results of such calculations are used to provide tentative explanations for the preference of the two conformers for centrosymmetric and non-centrosymmetric space groups. Several comments on general problems encountered in crystal structure prediction are also presented, concerning in particular the multi-minima structure of the potential energy hypersurface.

## 1. Introduction

The polymorphism of the title compound has been recently studied by single-crystal X-ray diffraction (Jasinski & Woudenberg, 1995). The case is particularly attractive from a theoretical standpoint, for a number of reasons: (*a*) two polymorphic forms were found in the same crystal crop; (*b*) one polymorph is centrosymmetric, the other non-centrosymmetric, and differences in optical properties were found; (*c*) neither polymorph adopts space group $P2_1/c$, by far the favourite for organic compounds (see *e.g.* Brock & Dunitz, 1994); (*d*) the molecular conformation in the two phases is slightly different, one molecule (in *Pbca*) being quite flat, the other (in $Pna2_1$) having a small twist along the flexible five-membered ring; and, last but not least, (*e*) reliable potentials for the calculation of lattice energies of such compounds are available (Filippini & Gavezzotti, 1993).

The structural and energetic data for the two X-ray structures are compared first, also in the light of recent studies on the general problem of polymorphism in organic crystals (Gavezzotti & Filippini, 1995). Then, a crystal structure generation procedure is applied to obtain virtual (*i.e.* computer-generated) crystal structures for both conformers in the centrosymmetric space group $P2_1/c$ and in non-centrosymmetric space groups $P2_12_12_1$, $P2_1$ and $Pna2_1$. The aim is to obtain some insight into the general problem of the choice of packing patterns of organic molecules, including conformational flexibility.

## 2. Analysis of the X-ray structures

Molecular models for the two conformers were constructed using the intramolecular geometry taken from the X-ray work, H atoms being located, as usual (Filippini & Gavezzotti, 1993), by geometrical criteria at 1.08 Å from their C atoms. A staggered conformation was imposed on the methyl groups. A molecular scheme with atomic numbering is given in Fig. 1, while the relevant structural and energetic data are collected in Table 1. As a reminder of the conformational difference, all data pertaining to the *Pbca* and $Pna2_1$ structures are labelled as FLAT and TWIST, respectively. Fig. 2 shows packing diagrams for the two structures, where two similar columnar motifs are seen.

Neither structure has particularly short intramolecular contacts and no sign of special polar interactions (*e.g.*

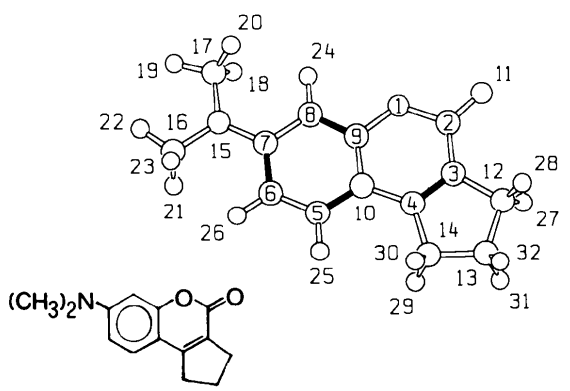


Fig. 1. Molecular scheme with atomic numbering. The molecule in both forms is essentially planar, but the FLAT conformer (*Pbca*) has a flat five-membered ring, the TWIST conformer ($Pna2_1$) has a 9.6(5)° twist along the C12—C13 bond and a −9.4(5)° twist along the C14—C13 bond (Jasinski & Woudenberg, 1995).

Table 1. *Structural and energetic data for the original crystal structures*

Cell parameters in Å, density in Mg $m^{-3}$, PE, packing energy, in kJ $mol^{-1}$.

| Structure | *a* | *b* | *c* | $V_{cell}$ | Density | PE |
|---|---|---|---|---|---|---|
| FLAT *Pbca* (X-ray) | 21.937 | 15.327 | 6.924 | 2328 | 1.307 | 129 |
| FLAT *Pbca* (relaxed) | 21.87 | 14.76 | 6.86 | 2216 | 1.373 | 133 |
| TWIST $Pna2_1$ (X-ray) | 8.779 | 22.042 | 6.043 | 1169.3 | 1.302 | 122 |
| TWIST $Pna2_1$ (relaxed) | 8.90 | 21.50 | 5.86 | 1120 | 1.359 | 124 |

short C=O···C or C=O···H distances; Gavezzotti, 1991*a*) appears. This justifies our using, in the crystal energy hypersurface search, empirical intermolecular potentials (Filippini & Gavezzotti, 1993) calibrated to reproduce thermodynamic and structural features of crystals containing non-polar or moderately polar molecular fragments, without including explicit coulombic terms, since electrostatic contributions have been shown to be well reproduced (at least for these compounds) by 6-exp potentials alone. However, the modulating effects of the introduction of point charges were analysed (see *Discussion*).

The density difference between the two phases is very small (0.5%), while the packing energy difference is more significant (6%) in favour of the denser phase: this is normal behaviour in polymorphic couples (Gavezzotti & Filippini, 1995). Thus, the non-centrosymmetric crystal has a lower packing energy and is therefore less stable on the intermolecular side; the difference in intramolecular energy between the two conformers may compensate in part for this. No attempt to calculate this conformational energy difference was however made, since it is unlikely that structure optimization for the isolated molecules could yield two separate minima for such a small difference in torsion angles along a flexible cyclic chain, while calculations of conformational energies at frozen geometries usually yield unreliable results, when parametric methods are used (quantum mechanical methods of sufficient accuracy are out of the question for such a large molecule). A rough guess, based on torsional potentials with a barrier height of 12 kJ $mol^{-1}$, as in ethane, yields *ca* 3 kJ $mol^{-1}$ in favour of the TWIST conformer.

For comparison with calculated crystal structures, the X-ray structures were subjected to structure relaxation (Williams, 1983) under the action of the intermolecular potentials. As expected, the relaxation of cell parameters was small (see Table 1), confirming the adequateness of the potentials. Rigid-body angular displacements were 1.5 and 3.1°, centre-of-mass shifts were negligible and the usual cell volume shrinkage (less than 5%) resulted, well within the acceptable limits (Gavezzotti & Filippini, 1995).

Most likely, the flexible five-membered ring adopts in solution a number of different conformations. In the centrosymmetric crystal structure, molecules form tight dimers over an inversion centre, being apparently squeezed to a fully planar conformation, and the thermal factor of C13, the outmost atom of the five-membered ring, is not particularly large. In the non-centrosymmetric structure there are no molecular pairs in close contact and C13 is apparently more free to librate (its $U_{eq}$ is twice the average), thus allowing the five-membered ring to relax to a more favourable, slightly twisted conformation.

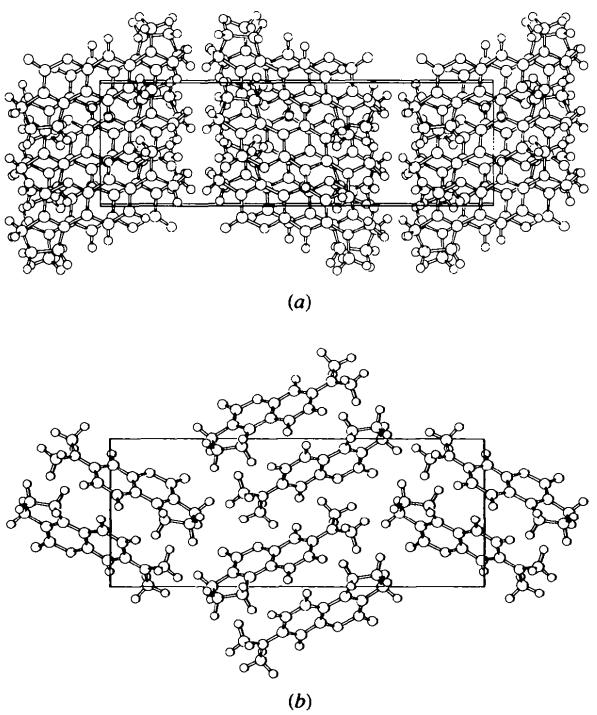

(*a*)

(*b*)

Fig. 2. (*a*) *Pbca* and (*b*) $Pna2_1$ structures for the title compound (after Jasinski & Woudenberg, 1995). Graphics by the program *SCHAKAL92* (Keller, 1993).

## 3. Crystal structure search

Both the FLAT and TWIST conformer were packed with frozen geometry in space groups $P2_1/c$, $P2_1$, $P2_12_12_1$ and $Pna2_1$. The essentials of the method are described in Gavezzotti (1991*b*), while the computer program used includes a number of updates and ameliorations that render it much faster and more efficient in the structure search (Gavezzotti, 1994*a*,*b*). The procedure does not allow so far the consideration of space groups with more than four molecules in the cell, so that no search could be conducted in *Pbca*. Structures generated by the *PROMET*3 (Gavezzotti, 1994*a*) procedure were accepted when having a packing coefficient higher than 0.55 and a substantially cohesive packing energy; these were then optimized in a final stage by a very efficient second-derivative crystal packer (Williams, 1983) and each should therefore represent a minimum in the crystal energy hypersurface.

### 3.1. *The $P2_1/c$ search*

For this search, centrosymmetric dimers were first generated, with distances between centres-of-mass of the two partners ranging from 4.0 to 5.9 Å. A screw axis was then added, with variable distances from the dimer and variable orientation; the cell periodicity along this axis ranging from 4 to 14 Å. The resulting glide plane displacement (the product of the first two operators) was allowed to reach a maximum length of 12 Å (cell periodicity 24 Å). The structural entity obtained in this way is termed a layer; it is, in fact, the *yz* layer in $P2_1/c$. Layers having a cohesion energy $\sim 20\%$ of that of the most stable known polymorph were deemed acceptable. A search was then conducted for accepted layers on the length and direction of the remaining cell periodicity, *a*, thus also determining the $\beta$ angle. For reference, the computing time was around 48 CPU h on a Silicon Graphics Indy workstation and can thus be classified as almost negligible on modern standards.

### 3.2. *The $P2_1$ search*

Around a screw operator, placed at variable distances from the molecule and with variable orientations, molecular strings were constructed with a screw pitch ranging from 2 to 7 Å (cell periodicity 4–14 Å). Acceptance criteria for these strings were set at a generous (*i.e.* very small) percentage of the packing energy. Subsequent structure expansion steps on accepted strings were performed to construct full three-dimensional structures by varying the *a*- and *c*-cell periodicities and the $\beta$ angle within suitable ranges.

### 3.3. *The $P2_12_12_1$ search*

The same strings defined for the $P2_1$ search were used and a second screw operator, perpendicular to the first and at a variable distance from it, was applied, resulting in full three-dimensional crystal structures, since the parameters of the third screw operator, as well as the cell periodicities, are completely determined once the pitch and the relative position of the first two screw axes are determined.

### 3.4. *The $Pna2_1$ search*

The screw strings previously considered for $P2_1$ were used, adding a glide operator with the appropriate orientation for the generation of this space group. Other details are as for space group $P2_12_12_1$.

## 4. Results and discussion

Tables 2 and 3 summarize the main numerical results, while Figs. 3–6 provide some (visually more impressive) graphical display. Fig. 3 shows a scattergram of the packing energy (PE) *versus* cell volume; there is an obvious broad correlation between these two quantities.

Table 2. *Number of crystal structures found, by space group and energy range*

| Structure | Packing energy range (kJ mol$^{-1}$) 130–132 | 126–130 | 121–126 | 117–121 |
|---|---|---|---|---|
| FLAT $P2_1/c$ | 1 | 20 | 82 | 110 |
| TWIST $P2_1/c$ | 0 | 8 | 43 | 69 |
| FLAT $P2_1$ | 0 | 0 | 16 | 61 |
| TWIST $P2_1$ | 0 | 0 | 13 | 52 |
| FLAT $P2_12_12_1$ | 0 | 3 | 18 | 36 |
| TWIST $P2_12_12_1$ | 0 | 4 | 17 | 39 |
| FLAT $Pna2_1$ | 0 | 0 | 4 | 12 |
| TWIST $Pna2_1$ | 0 | 1 | 4 | 8 |

Figs. 4 and 5 show the scattergram of PE against the *b*- and *c*-cell axes; of course, in the different space groups these axes have different meanings as regards uniqueness and direction of the relevant symmetry operators. The monoclinic screw periodicity (*b* axis) shows an aggregation in the 7–8 Å range, not far from the 6.0 Å screw in $Pna2_1$ and the 6.9 Å screw in *Pbca*. The *c*-axis periodicity shows aggregations around 15 and 24 Å, to be compared with the 15.3 and 21.9 glide directions in *Pbca*, and with the 22.9 glide direction in $Pna2_1$. 4 Å axes are always present, resulting from pure stacking of flat molecules at contact distances. Fig. 6 shows the same plot for the $\beta$ angle in monoclinic space groups; the approximate mirror symmetry around 90° results from the redundancy of the search procedure.

The most impressive feature of all these plots is the spread of the structural parameters obtained once PE decreases by a few per cent from the most favourable value. For example, the *b*-axis length in the monoclinic structures of the FLAT conformer is selective for PE below $-130$ kJ mol$^{-1}$, relaxes a little if PE rises to $-125$ kJ mol$^{-1}$ and becomes totally unselective (*b*

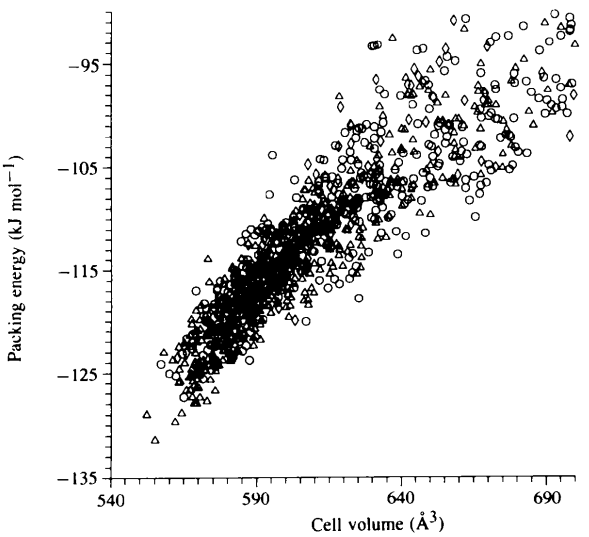


Fig. 3. Packing energy against cell volume for calculated crystal structures, FLAT conformer. The scattergram for the other conformer is similar. Circles: $P2_1$, triangles: $P2_1/c$, squares: $P2_12_12_1$, rhombuses: $Pna2_1$.

Table 3. *Structural and energetic data for the most stable computer-generated crystal structures*

Cell parameters in Å and °, cell volume per molecule, packing energy in kJ mol$^{-1}$; $S$ is the damping factor applied to Extended Hückel charges ($S = \infty$ indicates no charges). Labels are for identification during the discussion.

| Structure | $a$ | $b$ | $c$ | $\beta$ | $V_{cell}$ | Packing energy $S = \infty$ | $S = 6.5$ | $S = 3.0$ | Label |
|---|---|---|---|---|---|---|---|---|---|
| FLAT *Pbca* | 21.87* | 14.76 | 6.86 | – | 554 | 133 | 141 | 152 | – |
| FLAT $P2_1$ | 7.49 | 4.02 | 18.65 | 83 | 557 | 124.1 | 132 | – | *F*4 |
| | 7.46 | 6.91 | 11.31 | 83 | 579 | 124.1 | 131 | 140 | *F*5 |
| | 14.28 | 6.91 | 7.42 | 52 | 576 | 123.9 | – | – | – |
| FLAT $P2_1/c$ | 7.96 | 6.77 | 22.12 | 112 | 555 | 131.3 | 140 | 151 | *F*2 |
| | 7.25 | 7.91 | 22.05 | 63 | 562 | 129.6 | 138 | 149 | *F*3 |
| | 7.21 | 7.89 | 20.29 | 102 | 564 | 128.7 | – | – | – |
| FLAT $P2_12_12_1$ | 20.73 | 3.98 | 13.86 | – | 571 | 125.6 | 132 | 137 | *F*6 |
| | 14.18 | 5.30 | 14.95 | – | 562 | 125.3 | 133 | 144 | *F*7 |
| | 13.31 | 4.87 | 17.63 | – | 572 | 124.6 | – | – | – |
| | 21.52 | 7.15 | 7.64 | – | 587 | 123.8 | – | – | – |
| FLAT $Pna2_1$ | 13.07 | 21.70 | 4.03 | – | 571 | 124.1 | 130 | 138 | *F*8 |
| | 9.09 | 21.35 | 5.80 | – | 563 | 123.5 | 131 | 142 | *F*9 |
| | 11.35 | 25.05 | 4.01 | – | 570 | 124.1 | – | – | – |
| TWIST $Pna2_1$ | 8.86* | 21.49 | 5.88 | – | 560 | 124.6 | 132 | 144 | *T*8 |
| | 12.63 | 22.04 | 4.05 | – | 564 | 126.2 | 131 | 134 | *T*5 |
| TWIST $P2_1$ | 7.48 | 4.12 | 18.41 | 91 | 567 | 124.4 | 130 | 134 | *T*6 |
| | 7.18 | 6.31 | 12.77 | 84 | 575 | 122.8 | 131 | 145 | *T*7 |
| | 6.89 | 5.55 | 15.00 | 90 | 573 | 121.2 | – | – | – |
| | 6.37 | 11.87 | 7.72 | 96 | 581 | 120.6 | – | – | – |
| TWIST $P2_1/c$ | 8.04 | 6.86 | 21.84 | 69 | 562 | 127.8 | 136 | 148 | *T*1 |
| | 10.85 | 7.12 | 14.67 | 93 | 566 | 127.0 | 134 | 143 | *T*2 |
| | 6.91 | 7.49 | 23.11 | 108 | 568 | 127.0 | – | – | – |
| | 7.75 | 11.22 | 14.74 | 62 | 565 | 124.1 | – | – | – |
| TWIST $P2_12_12_1$ | 13.28 | 4.07 | 20.93 | – | 566 | 128.7 | 135 | 144 | *T*3 |
| | 21.82 | 6.92 | 7.50 | – | 566 | 126.6 | 134 | 142 | *T*4 |

* X-ray structures.

ranging from 4 to 14 Å) as PE rises above $-125$ kJ mol$^{-1}$, or a 4% difference from the most stable structure. A wide sea of hundreds of crystal structures can be seen in these plots, all close-packed and acceptable (ignoring the selective part of the graph), waiting for some driving force leading to the unique, or nearly unique, best structure; perhaps a model or a reminiscence of the fluxional pre-crystallization multinuclear phase.

To resolve at least in part the redundancy of the search, two structures were considered equal when differing by less than 3% in cell periodicities and 2% in packing energy. The increasing number of structures found as PE lowers is evident (Table 2). Table 3 shows details of the best structures; a deposited table contains full atomic coordinates for the two best structures in each space group.*

To assess the role of $R^{-1}$ terms in modulating the results, the standard potentials were supplemented by such terms computed over point-charge parameters located at atomic nuclei and calculated by Mulliken population analysis on an Extended Hückel (Hoffmann, 1963) wavefunction (see Gavezzotti & Filippini, 1994 for further details; a damping factor of 6.5 or 3.0 was applied to the raw Mulliken charges). The packing energies of the best structures were recalculated (Williams, 1983; forced convergence options fully applied) with these modified potentials and the results are also shown in Table 3.

The *Pbca* structure of the FLAT conformer is more stable than any other structure, although differences with $P2_1/c$ are marginal. This result is insensitive to $R^{-1}$ terms in the potential – an encouraging result as regards the performance of the potential field. For the TWIST conformer, the X-ray $Pna2_1$ structure was unequivocally located during the structure search, confirming that the *PROMET*3 procedure is adequate for the solution of the phase problem in X-ray crystallography, when molecular conformation is predetermined; biasing the search by the known cell parameters and space group easily leads to the correct solution (of course, the impact of this news on the crystallographic community would have been much greater 20 years ago). The same $Pna2_1$ structure is also possible for the FLAT conformer.

The introduction of $R^{-1}$ terms enhances the relative stability of the $Pna2_1$ structure, but no structural rearrangement occurs after their introduction; structures predicted without these terms are unchanged, the energy balance being affected in a static way by the addition of subtle modulating amounts to the packing energy. This result is encouraging as regards the application of crystal structure search procedures without the time-consuming $R^{-1}$ terms, only a final fine-tuning of the total energies being required.

* A list of atomic coordinates for the two most stable calculated structures in each space group has been deposited with the IUCr (Reference: NA0070). Copies may be obtained through The Managing Editor, International Union of Crystallography, 5 Abbey Square, Chester CH1 2HU, England.

Yet, for the TWIST conformer one $P2_1/c$ structure was calculated to be the most stable of all in all circumstances, being pretty much the same as the best one for the FLAT conformer; therefore, this structure is possible for both conformers, being marginally less stable than that observed for the FLAT conformer, and significantly more stable than that observed for TWIST. The reason for the appearance of the $Pna2_1$ structure must be some sort of non-centrosymmetric induction at the nucleation stage, presumably of electrostatic origin; otherwise, the TWIST conformer would pick up the favourable $P2_1/c$ structure. Then, the reasons for discrimination between $Pna2_1$, $P2_1$ and $P2_12_12_1$ are not clear (their energies being quite close, see Table 3).

Clearly, a more in-depth structural analysis than just comparisons of cell parameters and packing energies is required. We will make sparing use of graphics (always somewhat deceiving) and more substantial use of quantitative overall structure descriptors, the so-called structural determinants, derived as follows. The total lattice energy is partitioned into contributions ($E_j$) between a reference molecule and each of the surrounding ones. The coordination sphere is defined as the collection of $N$ molecules for which $E_j > 5\%$ of the total

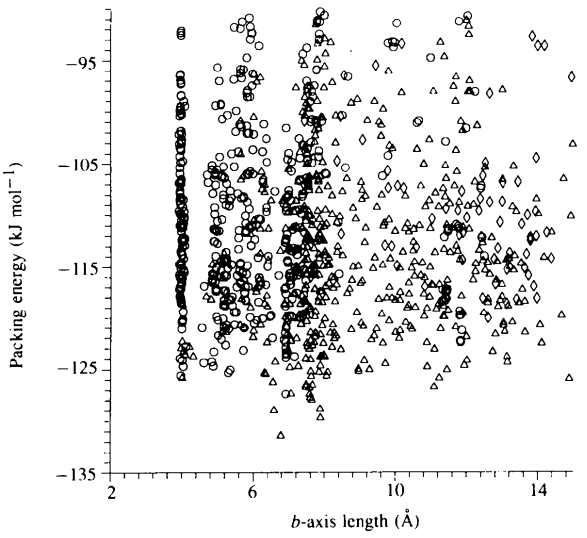


(*a*)

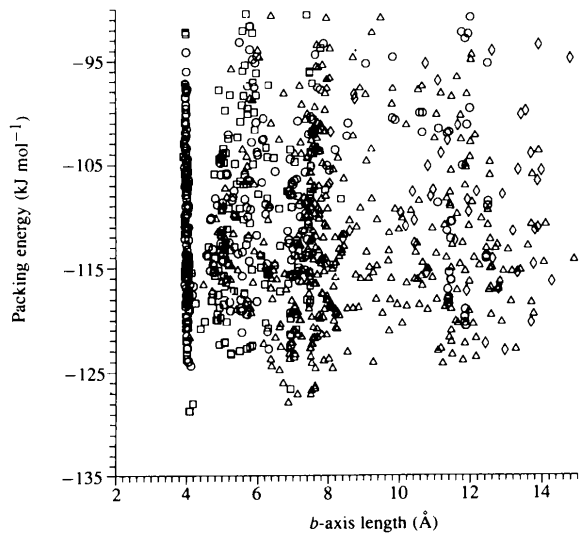


(*b*)

Fig. 4. Distribution of *b*-axis lengths in calculated structures. (*a*) FLAT and (*b*) TWIST conformers.

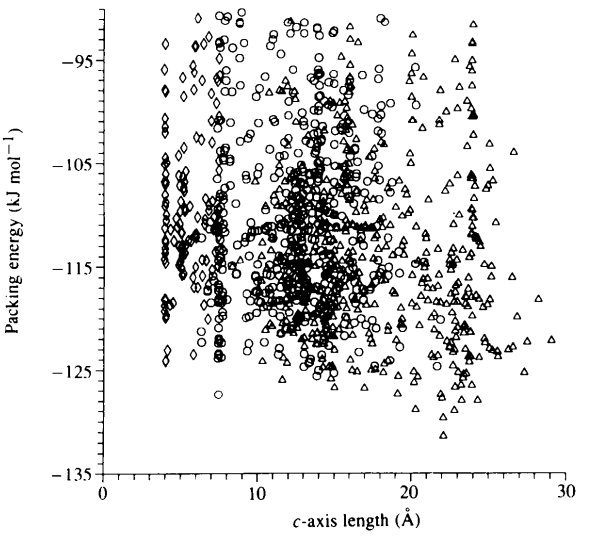


Fig. 5. Distribution of *c*-axis lengths in calculated structures, FLAT conformer.

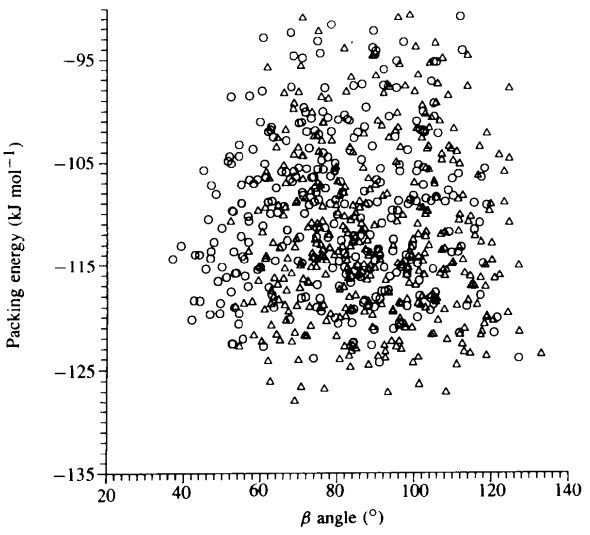


Fig. 6. Distribution of $\beta$ angles in calculated monoclinic structures.

lattice energy; each of these molecules is also identified by a symmetry operator, $O_j$, by which it is related to the reference one, by the distance, $R_j$, between its centre-of-mass and that of the reference one, and by the angle, $\theta_j$, between the molecular planes – clearly identifiable in a flat molecule. A structure determinant can then be written as:

$$N;\ (E_1, O_1, R_1, \theta_1), (E_2, O_2, R_2, \theta_2), \ldots (E_N, O_N, R_N, \theta_N).$$

Table 4 shows the results of this type of analysis. The *Pbca* structure and the two $P2_1/c$ structures $F2$ and $T1$ contain the same dimer over a centre of symmetry, but for the TWIST conformer this dimer is less stable (65 against 71 kJ mol$^{-1}$) than for the FLAT conformer; a point in favour of the speculation (see above) of non-centrosymmetric induction within the solution. The *Pbca* structure then adopts a T-shaped motif with molecules aligned with their long molecular axes parallel at an interplanar angle of 59° (Fig. 7*a*), which is absent in the

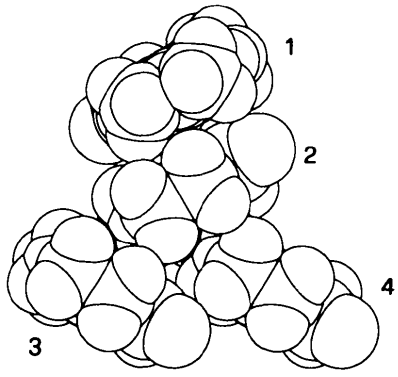


(*a*)

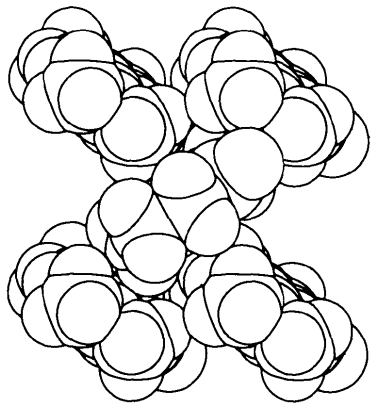

(*b*)

Fig. 7. The basic packing motifs; (*a*) *Pbca* structure, molecules 1 and 2 in the centrosymmetric dimer, molecules 3 and 4 in the propagating herringbone pattern; (*b*) $Pna2_1$ structure, the quincunx-like herringbone arrangement. Graphics by the program *SCHAKAL*92 (Keller, 1993).

Table 4. *Structure determinants*

The entries for each line are: operator symbol (I = inversion center, S = screw dyad, G = glide, T = translation), distance between centres-of-mass (Å), molecule–molecule energy (kJ mol$^{-1}$), interplanar angle (°); see text. Structure labels as in Table 3.

| | | | | | | | | | | | | |
|---|---|---|---|---|---|---|---|---|---|---|---|---|
| | FLAT *Pbca* | | | | *F*2 | | | | *T*1 | | | |
| I | 3.81 | −71 | – | | I | 3.73 | −71 | – | I | 3.85 | −65 | – |
| 2G | 5.39 | −36 | 59 | | I | 4.27 | −55 | – | I | 4.23 | −56 | – |
| 2T | 6.92 | −19 | – | | 2T | 6.77 | −20 | – | 2T | 6.86 | −18 | – |
| I | 7.59 | −17 | – | | I | 7.40 | −17 | – | I | 7.53 | −18 | – |
| | TWIST $Pna2_1$ | | | | *F*9 | | | | *T*8 | | | |
| 2S | 6.72 | −33 | 69 | | 2S | 6.73 | −32 | 74 | 2S | 6.69 | −33 | 72 |
| 2S | 5.40 | −33 | 69 | | 2S | 5.33 | −33 | 74 | 2S | 5.31 | −33 | 72 |
| 2T | 6.04 | −23 | – | | 2T | 5.80 | −25 | – | 2T | 5.88 | −24 | – |
| | *F*3 | | | | *T*2 | | | | | | | |
| I | 3.94 | −65 | – | | I | 3.91 | −66 | – | | | | |
| I | 6.33 | −41 | – | | I | 4.50 | −63 | – | | | | |
| I | 6.57 | −20 | – | | 2G | 7.34 | −17 | 22 | | | | |
| 2S | 8.86 | −18 | 51 | | | | | | | | | |
| | *F*5 | | | | *T*4 | | | | | | | |
| 2S | 3.94 | −65 | 0 | | 2S | 3.92 | −65 | 0 | | | | |
| 2S | 6.84 | −16 | 0 | | 2S | 6.85 | −16 | 0 | | | | |
| 2S | 7.46 | −16 | 0 | | 2T | 7.50 | −16 | – | | | | |
| | *F*4 | | | | *T*6 | | | | | | | |
| 2T | 4.02 | −62 | – | | 2T | 4.12 | −60 | – | | | | |
| 2T | 7.49 | −15 | – | | 2T | 7.48 | −16 | – | | | | |
| | *F*6 | | | | *T*3 | | | | | | | |
| 2T | 3.98 | −62 | – | | 2T | 4.07 | −63 | – | | | | |
| 2S | 8.90 | −14 | 60 | | 2S | 7.58 | −17 | 24 | | | | |
| | | | | | 2S | 7.05 | −16 | 24 | | | | |
| | *F*8 | | | | *T*5 | | | | | | | |
| 2T | 4.03 | −62 | – | | 2T | 4.05 | −63 | – | | | | |
| 2G | 7.96 | −17 | 3 | | 2G | 7.75 | −13 | 55 | | | | |
| | *F*7 | | | | *T*7 | | | | | | | |
| 2T | 5.30 | −53 | – | | 2T | 6.31 | −44 | – | | | | |
| 2S | 6.83 | −17 | 82 | | 2S | 7.25 | −20 | 69 | | | | |
| | | | | | 2T | 7.18 | −14 | – | | | | |
| | | | | | 2S | 8.10 | −13 | 69 | | | | |

$P2_1/c$ structures. The $F2$ and $F3$ structures are other variations on the same dimer theme (Fig. 8).

The $Pna2_1$ structure, found by X-rays for TWIST and by calculation for both TWIST and FLAT, has a basic herringbone motif similar to that found in the *Pbca* structure, but with a larger interplanar angle (69 against 59°; Fig. 7*b*). In the calculated non-centrosymmetric structures, the substitute for the centrosymmetric dimer is either a stacked translation motif with a repeat distance of 4 Å ($F4$ and $T6$, $F6$ and $T3$, $F8$ and $T5$; see Fig. 9) or a screw stacking motif in which the twofold axis is perpendicular to the molecular plane and bisects approximately through the centre-of-mass, while the screw dislocation is just 4 Å ($F5$ and $T4$; for a perfectly planar figure, the inversion centre and such a twofold axis have the same effect). This device is never quite as effective as the true centre of symmetry, since $E_j$s are invariably slightly smaller. The two structures $F7$ and $T7$ have instead a peculiar herringbone pattern without any 4 Å interplanar separations (see Fig. 10).

## 5. Concluding remarks

### 5.1. *The case under study*

A likely interpretation of the nucleation and crystallization process for the title molecule, on the basis of the above results, is as follows. The most stable packing pattern originates from a centrosymmetric dimer whose cohesive power is large enough to force the molecule to flatten its five-membered ring. Dimers then pack in the herringbone fashion obtained in *Pbca* (Fig. 7*a*). At nucleation time, however, molecules still have conformational freedom; if a twisted conformation on the ring is preserved, the centrosymmetric dimer becomes less stable and a non-centrosymmetric driving force of electrostatic origin has a chance to manifest itself in the pure herringbone packing exhibited in $Pna2_1$ (Fig. 7*b*).

### 5.2. *Further remarks*

The case study described in this paper, without actually tackling the problem of full *ab initio* crystal structure prediction for organic compounds (Gavezzotti, 1994*b*), focuses on some of its features and turning points. We illustrate the power of the crystal structure generation procedure embodied in the *PROMET*3 code; we cannot claim it is superior to molecular dynamics approaches (Karfunkel & Gdanitz, 1992), but at least find no evidence that it is largely inferior. It allows for geometrical crystallography and symmetry relationships as input, instead of reckoning them from output; this appeals to the crystallographer, rather than to the general computational chemist, and is a strong point in that it permits educated guesses based on crystal chemistry, but a weak point also inasmuch as it introduces some restrictions on the search. The fact that such a procedure leads to a way of solving the phase problem in X-ray

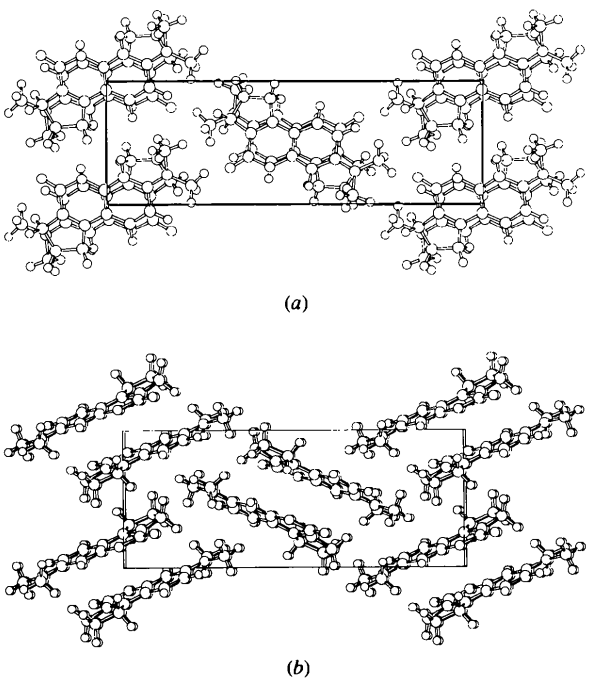

(*a*)

(*b*)

Fig. 8. Two $P2_1/c$ structures: (*a*) *F*2, similar to *T*1, and (*b*) *F*3, similar to *T*2. Graphics by the program *SCHAKAL*92 (Keller, 1993).

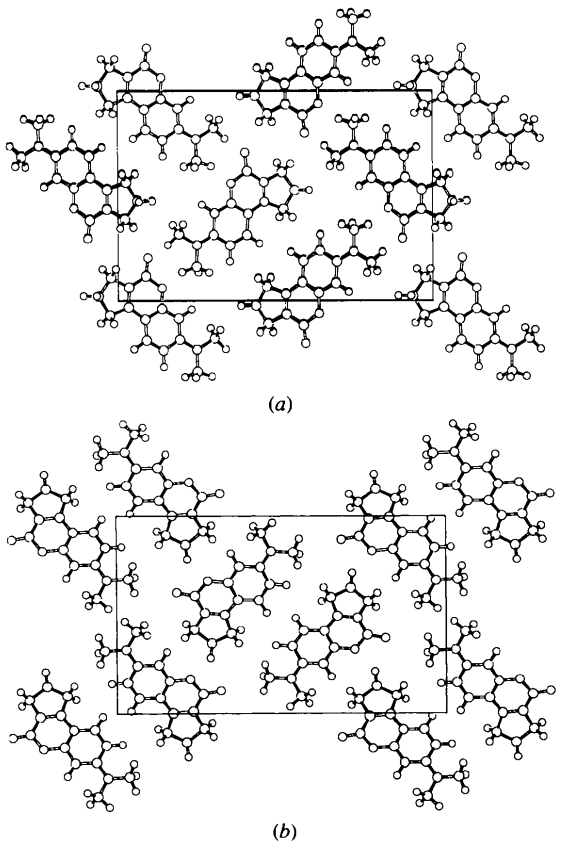

(*a*)

(*b*)

Fig. 9. (*a*) $P2_12_12_1$ structure *F*6, similar to *T*3, and (*b*) $Pna2_1$ structure *F*8, similar to *T*5. Graphics by the program *SCHAKAL*92 (Keller, 1993).

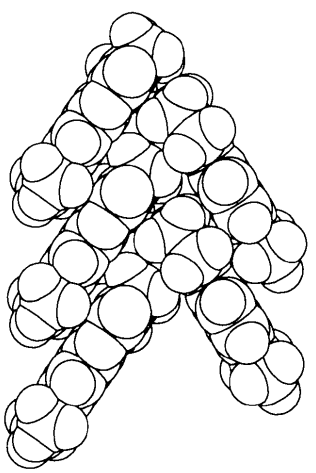

Fig. 10. The herringbone motif in the $P2_12_12_1$ structure *F*7, similar to *T*7. Graphics by the program *SCHAKAL*92 (Keller, 1993).

crystallography comes too late to be of any practical use in a general sense, but may be useful in some peculiar cases.

As in previous experience (see *e.g.* van Eijck, Mooij & Kroon, 1995), we find a wealth of crystal structures, with different space groups and packing patterns, all enclosed within an interval of *ca* 10 kJ mol$^{-1}$ of lattice energy. The use of quantitative structure determinants, rather than elusive graphical methods, in crystal structure comparisons, is advocated. These determinants identify a structure better than many other indicators, in many ways overcoming the problems related to the non-uniqueness of cell and space group choices. Structures judged to be different on these last premises may turn out to be quite similar in the packing motif.

Empirical atom–atom force fields without the introduction of $R^{-1}$ terms perform reasonably in the structure screening stage. The introduction of these terms can be instrumental when screening the finer details of relative structure stabilities, in particular that which concerns the well known, much discussed but as yet unsettled matter of the stacking *versus* edge-to-core arrangement of aromatic moieties. Still, the energy of many calculated crystal structures is almost equal to that of the structures found experimentally, so that this finer detail remains beyond the reach of present-day structure search procedures, whose resolving power seems to be at least one order of magnitude lower than necessary for unequivocal crystal structure prediction. Moderate conformational flexibility, which is the case in the present structure, of course adds to the complexity of the problem (perhaps more than larger conformational differences, where one is actually dealing with several different molecular entities). A strategy for crossing the sea of tens or hundreds of close-packed, wrong crystal structures to the equally close-packed correct one calls for better physics in the force fields, for subtler and more powerful hypersurface search algorithms, as well as for a better understanding of the nucleation phenomenon.

Financial support from MURST is gratefully acknowledged.

## References

Brock, C. P. & Dunitz, J. D. (1994). *Chem. Mater.* **6**, 1118–1127.
Eijck, B. P. van, Mooij, W. T. & Kroon, J. (1995). *Acta Cryst.* B**51**, 99–103.
Filippini, G. & Gavezzotti, A. (1993). *Acta Cryst.* B**49**, 868–880.
Gavezzotti, A. (1991*a*). *J. Phys. Chem.* **95**, 8948–8955.
Gavezzotti, A. (1991*b*). *J. Am. Chem. Soc.* **113**, 4622–4629.
Gavezzotti, A. (1994*a*). *PROMET*3. *A Program for the Generation of Possible Crystal Structures from the Molecular Structure of Organic Compounds*. University of Milano (available from the author upon request).
Gavezzotti, A. (1994*b*). *Acc. Chem. Res.* **27**, 309–314.
Gavezzotti, A. & Filippini, G. (1994). *J. Phys. Chem.* **98**, 4831–4837.
Gavezzotti, A. & Filippini, G. (1995). *J. Am. Chem. Soc.* In the press.
Hoffmann, R. (1963). *J. Chem. Phys.* **39**, 1397–1412.
Jasinski, J. P. & Woudenberg, R. C. (1995). *Acta Cryst.* C**51**, 107–109.
Karfunkel, H. R. & Gdanitz, R. (1992). *J. Comput. Chem.* **13**, 1171–1183.
Keller, E. (1993). *SCHAKAL*92. *A Program for the Graphic Representation of Molecular and Crystallographic Models*. University of Freiburg.
Williams, D. E. (1983). *PCK*83. QCPE Program 548. Quantum Chemistry Program Exchange, Chemistry Department, Indiana University, Bloomington, Indiana.